pp ELASTIC SCATTERING IN CONDENSATE-ENCLOSED CHIRAL-BAG MODEL AT 13 TeV*

M.M. ISLAM†, R.J. LUDDY‡

Department of Physics, University of Connecticut, Storrs, CT 06269, USA

(Received November 12, 2015)

At the 2011 Blois Workshop, pp elastic scattering measurements at the LHC at 7 TeV were presented by the TOTEM Collaboration. They showed that our predicted $d\sigma/dt$ in the momentum transfer region $|t| \simeq 0.5$–2.5 GeV^2 disagreed significantly with TOTEM results. This led us to consider an extensive investigation of the large $|t|$ pp elastic scattering that included: *(i)* multiple ω-exchanges; *(ii)* valence quark–quark scattering via low-x gluon–gluon interactions; and *(iii)* the single ω-exchange amplitude and the quark–quark scattering amplitude having opposite signs. We found a satisfactory description of the 7 TeV $d\sigma/dt$ in the region of $0.6\ \text{GeV}^2 < |t| < 2.5\ \text{GeV}^2$. This result was presented by us at the Blois 2013 Workshop. However, as noted by others, there was still a significant difference between our calculated $d\sigma/dt$ and TOTEM data in the forward direction: $|t| < 0.6\ \text{GeV}^2$. This led us to envisage a new aspect of our $q\bar{q}$ Condensate-Enclosed Chiral-Bag Model of the proton. In this model, the proton has a core of baryonic shell with valence quarks inside. The proton baryonic-charge core polarizes the $q\bar{q}$ condensate cloud and creates a layer of antiquarks surrounding the baryonic core. This, in turn, leads to a layer of positive quarks at the boundary of the proton. For an antiproton, the opposite happens — a layer of negative antiquarks appears at the boundary of the antiproton. In pp forward scattering, the two polarization layers at the boundary interact giving rise to a new scattering amplitude. For $\bar{p}p$, the same thing happens except the amplitude has the opposite sign as in D0 1.96 TeV. Our phenomenological investigation has now shown that we can describe quantitatively the pp $d\sigma/dt$ TOTEM data at 7 TeV throughout the entire $|t|$ range. We now predict the pp $d\sigma/dt$ at the LHC at 13 TeV, which will test our model of the proton structure.

DOI:10.5506/APhysPolBSupp.8.867

PACS numbers: 14.20.Dh

* Presented by M.M. Islam at EDS Blois 2015: The 16$^{\text{th}}$ Conference on Elastic and Diffractive Scattering, Borgo, Corsica, France, June 29–July 4, 2015.

† islam@phys.uconn.edu

‡ rjluddy@phys.uconn.edu

Our investigation of high-energy pp and $\bar{p}p$ elastic scattering over the last ten years has led us to the following physical picture of the proton (Fig. 1) [1–7]:

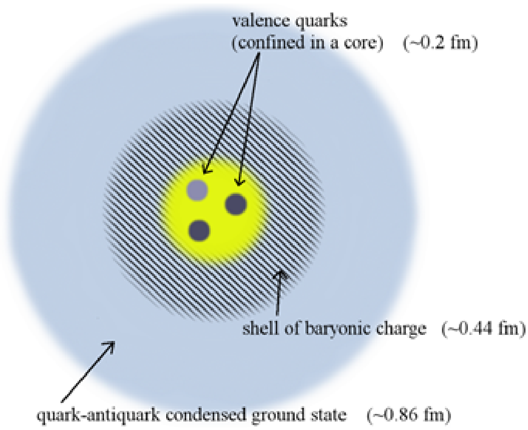

Fig. 1. Physical picture of the proton — a Condensate-Enclosed Chiral-Bag.

The proton has three regions: an outer region consisting of a quark–antiquark ($q\bar{q}$) condensed ground state; an inner shell of baryonic charge — where the baryonic charge is topological (or, geometrical); and a core of size 0.2 fm, where the valence quarks are confined. The part of the proton structure comprised of a shell of baryonic charge and three valence quarks has been known as "Chiral Bag" model of the nucleon in low-energy studies. What we are finding from high-energy elastic scattering is that the proton is a "Condensate-Enclosed Chiral-Bag".

The proton structure shown in Fig. 1 leads to three main processes in elastic scattering as shown in Fig. 2. The first process occurs in the small-$|t|$ region, *i.e.*, in the near forward direction, when the outer cloud of $q\bar{q}$ condensed ground state of one proton interacts with that of the other. It gives rise to diffraction scattering, which underlies: *(i)* the observed increase of the pp total cross section with energy: $\sigma_{\rm tot}(s) \sim (a_0 + a_1 \ln s)^2$, *i.e.*, qualitative saturation of the Froissart–Martin Bound (a_0, a_1 are parameters determined phenomenologically); *(ii)* it leads to $\rho(s) = \pi a_1/(a_0 + a_1 \ln s)$: ratio of the real part over the imaginary part of the forward scattering amplitude asymptotically; *(iii)* it is a crossing-even scattering amplitude, and therefore, yields equal pp and $\bar{p}p$ total cross sections.

The diffraction amplitude $T_{\rm D}^{+}(s,t)$ is represented by a profile function

$$T_{\rm D}^{+}(s,t) = ipW \int_0^\infty b\,db\,J_0(bq)\,\Gamma_{\rm D}^{+}(s,b)\,, \qquad (1)$$

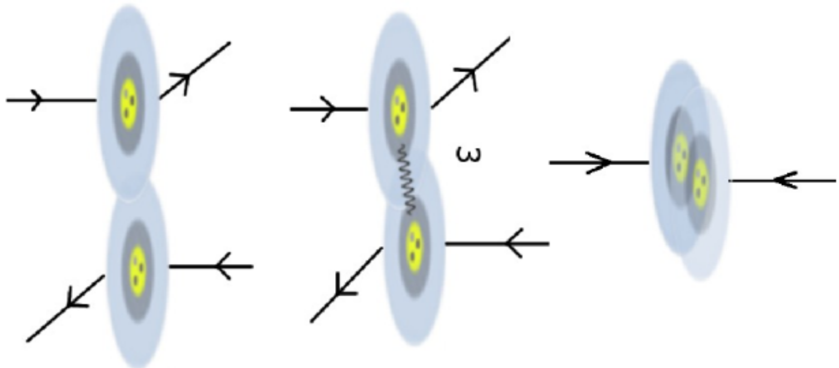

Fig. 2. Elastic scattering processes.

where the profile function $\Gamma_D^+(s,b)$ is taken to be

$$\Gamma_D^+(s,b) = g(s)\left[\frac{1}{1+\exp(b-R)/a} + \frac{1}{1+\exp(-(b+R)/a)}\right] . \tag{2}$$

$g(s)$ is a crossing-even function of s, $R = R(s) = R_0 + R_1(\ln s - i\frac{\pi}{2})$ and $a = a(s) = a_0 + a_1(\ln s - i\frac{\pi}{2})$. $\Gamma_D^+(s,b)$ can be expressed as

$$\Gamma_D^+(s,b) = g(s)\frac{\sinh\frac{R}{a}}{\cosh\frac{R}{a} + \cosh\frac{b}{a}} . \tag{3}$$

By changing the variable of integration from b to $\zeta = b/a$ and rotating the line of integration of ζ to the real axis [6], we obtain

$$T_D^+(s,t) = ipWa^2(s)g(s)\int_0^\infty \zeta d\zeta J_0(\zeta qa)\frac{\sinh\frac{R}{q}}{\cosh\frac{R}{a} + \cosh\zeta} . \tag{4}$$

At high energy, $a_0 + a_1 \ln s \to \infty$ and $\frac{R(s)}{a(s)} = \frac{R_0+R_1(\ln s - i\frac{\pi}{2})}{a_0+a_1(\ln s - i\frac{\pi}{2})} \simeq r$, where $r = R_1/a_1$ is a constant. To carry out further the integration on the right-hand side of Eq. (4), we replace $a(s)$ by $\hat{a}(s) = a_0 + a_1 \ln s$ in the integral and obtain

$$T_D^+(s,t) = ipW\left[a_0 + a_1\left(\ln s - i\frac{\pi}{2}\right)\right]^2 g(s)\int_0^\infty \zeta d\zeta J_0\left(\zeta q\hat{a}\right)\frac{\sinh r}{\cosh r + \cosh\zeta} , \tag{5}$$

where at high energy, $g(s)$ becomes a constant [1]

$$g_0 = (1 - \eta_0)\frac{1 + e^{-r}}{1 - e^{-r}} \,. \tag{6}$$

We note that — similar to the proton — the antiproton has a shell of anti-baryonic charge and a core of antiquarks. The quark–antiquark outer cloud of the antiproton, however, is exactly the same as the quark–antiquark outer cloud of the proton. So, the pp and $\bar{p}p$ diffraction scattering are the same: $T_{\mathrm{D}}^{+}(s,t)$ and there is no odd diffraction amplitude $T_{\mathrm{D}}^{-}(s,t)$.

Beyond diffraction scattering — the next dominant processes are multiple ω-exchanges and valence quark–quark scattering via low-x gluon–gluon interaction (Fig. 3). We also have to keep in mind that in pp and $\bar{p}p$ scattering — each ω-exchange is accompanied by a glancing collision of scalar particles of one proton (antiproton) with those of the other proton (Fig. 4).

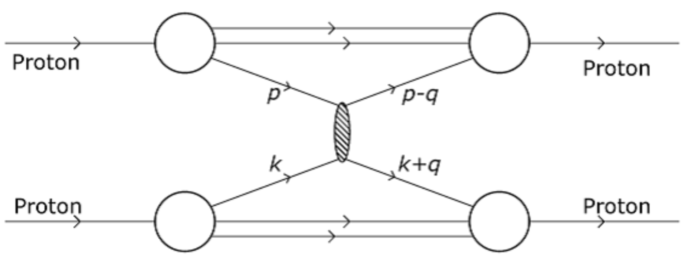

Fig. 3. Hard collision of a valence quark from one proton with one from the other proton.

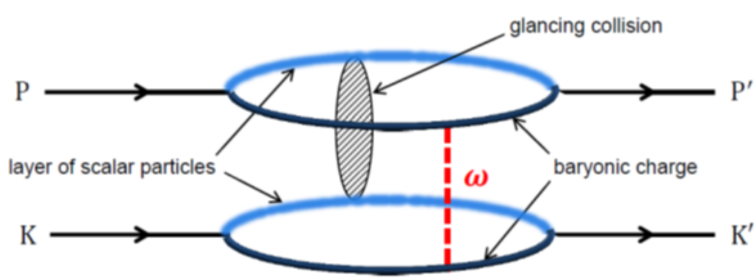

Fig. 4. Single ω-exchange accompanied by a glancing collision of scalar particles of one proton with those of the other proton (in momentum space).

The combined amplitude due to ω-exchanges and low-x gluon–gluon interaction can be expressed in terms of a joint eikonal: $\chi_\omega(s,b) + \chi_{gg}(s,b)$. The amplitude $T_{\omega+gg}(s,t)$ is, however, screened by diffraction scattering and by deep $q\bar{q}$ condensate close to the baryonic-charge shell. The resulting scattering amplitude is then

$$T_{\omega+gg}(s,t) = \left[\left(\eta_0 + \frac{c_0}{\left(se^{i\frac{\pi}{2}}\right)^\sigma}\right) + i\left(\lambda_0 - \frac{d_0}{s^2}\right)\right] ipW \int_0^\infty bdbJ_0(bq) \times \left[1 - e^{i(\chi_\omega(s,b)+\chi_{gg}(s,b))}\right], \quad (7)$$

where the first two terms on the right-hand side represent the screening effect.

Writing

$$\left[1 - e^{i(\chi_\omega(s,b)+\chi_{gg}(s,b))}\right] = \left[\left(1 - e^{i(\chi_\omega(s,b))}\right) + e^{i\chi_\omega(s,b)}\left(1 - e^{i(\chi_{gg}(s,b))}\right)\right], \quad (8)$$

we approximate Eq. (7) as

$$T_{\omega+gg}(s,t) \simeq \left[\left(\eta_0 + \frac{c_0}{\left(se^{i\frac{\pi}{2}}\right)^\sigma}\right) + i\left(\lambda_0 - \frac{d_0}{s^2}\right)\right] \times \left[T_\omega(s,t) + e^{i\chi_\omega(s,\tilde{b})} T_{gg}(s,t)\right]. \quad (9)$$

$T_\omega(s,t)$ is the scattering amplitude due to multiple ω-exchanges; $T_{gg}(s,t)$ is the gluon–gluon scattering amplitude (Fig. 3). $e^{i\chi_\omega(s,\tilde{b})}$ is an average value that shows the additional screening of the scattering amplitude $T_{gg}(s,t)$, because of the baryonic-charge shell.

We now examine $\bar{p}p$ scattering. As we have already observed, the same quark–antiquark cloud encloses an antiproton and a proton. So, the diffraction amplitude is $T_{\rm D}^{+}(s,t)$ for $\bar{p}p$ scattering as well. The combined amplitude due to ω-exchanges and low-x gluon–gluon interaction will now be expressed in terms of a joint eikonal: $\bar{\chi}_\omega(s,b) + \bar{\chi}_{gg}(s,b)$. The scattering amplitude is

$$\bar{T}_{\omega+gg}(s,t) = \left[\left(\eta_0 + \frac{c_0}{\left(se^{-i\frac{\pi}{2}}\right)^\sigma}\right) - i\left(\lambda_0 - \frac{d_0}{s^2}\right)\right] ipW \int_0^\infty bdbJ_0(bq) \times \left[1 - e^{i(\bar{\chi}_\omega(s,b)+\bar{\chi}_{gg}(s,b))}\right]. \quad (10)$$

Equation (10) can be further approximated as done earlier

$$\bar{T}_{\omega+gg}(s,t) \simeq \left[\left(\eta_0 + \frac{c_0}{\left(se^{-i\frac{\pi}{2}}\right)^\sigma}\right) - i\left(\lambda_0 - \frac{d_0}{s^2}\right)\right] \times \left[\bar{T}_\omega(s,t) + e^{i\bar{\chi}_\omega(s,b)} \bar{T}_{gg}(s,t)\right]. \quad (11)$$

We note that the explicit form of $T_{gg}(s,t)$ [7] is

$$T_{gg}(s,t) = is\gamma_{gg}\left(se^{-i\frac{\pi}{2}}\right)^{\lambda} \frac{F^2(q_\perp,\lambda)}{\left(1+\frac{q^2}{m^2}\right)^{2(\mu+1)}} \tag{12}$$

and $\bar{T}_{gg}(s,t) = T_{gg}(s,t)$, as they are crossing even.

In our study of pp and $\bar{p}p$ scattering, we have realized — a new scattering amplitude occurs. To see this, let us go back to Fig. 1, which shows that the proton has a shell of baryonic charge and a core of valence quarks — also of baryonic charge. They are enclosed by the quark–antiquark cloud. The cloud becomes polarized, because its antiquarks are drawn toward the baryonic shell. In turn, a layer of polarization quarks appear near the boundary (Fig. 5). In pp near forward scattering, the two outer layers collide leading to a new scattering amplitude (positive). In $\bar{p}p$ near forward scattering, the outer polarization layer of the antiproton is of antiquarks and the polarization scattering amplitude is negative.

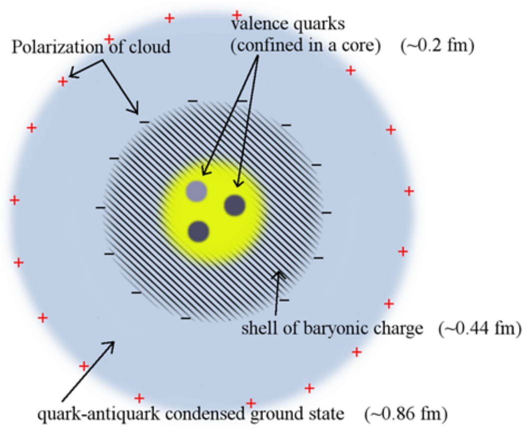

Fig. 5. Physical picture of the proton — a Condensate-Enclosed Chiral-Bag — with polarization of the cloud shown.

Our investigation has shown that the polarization amplitude $T_{\rm pl}(s,t)$ can be expressed in terms of a profile function

$$T_{\rm pl}(s,t) = ipW\int_0^\infty bdbJ_0(bq)\mathit{\Gamma}_{\rm pl}^{+,-}(s,b) \qquad (pp,\ \bar{p}p) \tag{13}$$

and we find a suitable profile function to be

$$\mathit{\Gamma}_{\rm pl}^{+,-}(s,b) = \pm Ae^{-b^2/B^2}J_0(bC) \qquad (pp,\ \bar{p}p) \tag{14}$$

with three parameters: A, B and C.

Our prediction for *pp* elastic $d\sigma/dt$ at 13 TeV is shown in Fig. 6, which will soon be measured at LHC by the TOTEM Collaboration. This measurement will establish how well we have predicted the 13 TeV *pp* $d\sigma/dt$ and determined the structure of the proton (Fig. 1).

Also shown in Fig. 6 is our calculated *pp* $d\sigma/dt$ at 7 TeV along with the TOTEM data. We include our calculated $\bar{p}p$ $d\sigma/dt$ at 1.96 TeV and present it with the D0 data and the earlier Tevatron $\bar{p}p$ 1.80 TeV data.

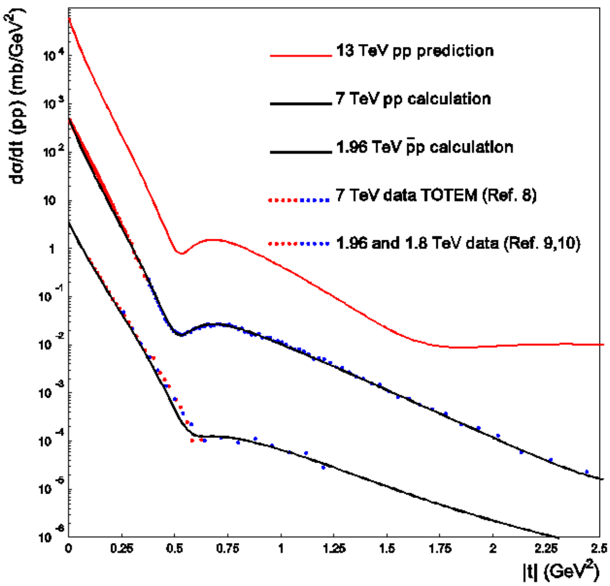

Fig. 6. Comparison of our $d\sigma/dt$ calculation at $\sqrt{s} = 7$ TeV with the TOTEM Collaboration measurements at the LHC [8]. Comparison of our $d\sigma/dt$ calculation at $\sqrt{s} = 1.96$ TeV with the D0 Collaboration and 1.8 TeV data [9,10]. Our $d\sigma/dt$ prediction at $\sqrt{s} = 13$ TeV — which is being measured by the TOTEM Collaboration at the LHC.

REFERENCES

[1] M.M. Islam, R.J. Luddy, A.V. Prokudin, *Int. J. Mod. Phys. A* **21**, 1 (2006).

[2] M.M. Islam, J. Kašpar, R.J. Luddy, Proc. of the 11$^{\rm th}$ Workshop on Non-Perturbative QCD, Paris 2011, ed. by B. Mueller, M.A. Rotondo, C.-I. Tan, `http://www.slac.stanford.edu/econf/C1106064/papers/Islam.pdf`

[3] I.M. Dremin, *Uspekhi* **56**, 3 (2013).

[4] J. Kašpar, V. Kundrát, M. Lokajíček, J. Procházka, *Nucl. Phys. B* **843**, 84 (2011).

[5] A. Hosaka, H. Toki, *Quarks, Baryons and Chiral Symmetry*, World Scientific, 2001.

[6] M.M. Islam, R.J. Luddy, A.V. Prokudin, *Mod. Phys. Lett. A* **18**, 743 (2003).

[7] M.M. Islam, J. Kašpar, R.J. Luddy, *Mod. Phys. Lett. A* **24**, 485 (2009).

[8] G. Antchev *et al.* [TOTEM Collaboration], *Europhys. Lett.* **95**, 41001 (2011); **101**, 21002 (2013).

[9] V.M. Abazov *et al.* [D0 Collaboration], *Phys. Rev. D* **86**, 012009 (2012).

[10] N.A. Amos *et al.*, *Phys. Lett. B* **247**, 127 (1990); F. Abe *et al.*, *Phys. Rev. D* **50**, 5518 (1994).